Synthesis, Characterization, and Morphology Studies of Biodegradable Amphiphilic Poly[(*R*)-3-hydroxybutyrate]-*alt*-Poly(ethylene glycol) Multiblock Copolymers

Xu Li,[†] Kerh Li Liu,[†,‡] Jun Li,[*,†,§] Eunice Phay Shing Tan,[§] Lee Meng Chan,[§] Chwee Teck Lim,[§] and Suat Hong Goh[‡]

Institute of Materials Research and Engineering (IMRE), National University of Singapore (NUS), 3 Research Link, Singapore 117602, Department of Chemistry, Faculty of Science, National University of Singapore (NUS), 3 Science Drive 3, Singapore 117543, and Division of Bioengineering and Department of Mechanical Engineering, Faculty of Engineering, National University of Singapore (NUS), 9 Engineering Drive 1, Singapore 117576, Singapore

Received July 13, 2006; Revised Manuscript Received August 28, 2006

Novel biodegradable amphiphilic alternating block copolymers based on poly[(*R*)-3-hydroxybutyrate] (PHB) as biodegradable and hydrophobic block and poly(ethylene glycol) (PEG) as hydrophilic block (PHB-*alt*-PEG) were successfully synthesized through coupling reaction. Their chemical structures have been characterized by using gel permeation chromatography, ^{1}H nuclear magnetic resonance, and Fourier transform infrared spectroscopy. Differential scanning calorimetry (DSC) analysis revealed that both PHB and PEG blocks in PHB-*alt*-PEG block copolymers can crystallize to form separate crystalline phase except in those with a short PEG block (M_n 600) only PHB crystalline phase has been observed. However, due to the mutual interference from each other, the melting transition of both PHB and PEG crystalline phases shifted to lower temperature with lower crystallinity in comparison with corresponding pure PHB and PEG. The crystallization behavior of PHB block and PEG block has also been studied by X-ray diffraction, and the results were in good agreement with those deduced from DSC study. The surface morphologies of PHB-*alt*-PEG block copolymer thin films spin-coated on mica have been visualized by atomic force microscopy with tapping mode, indicating formation of laterally regular lamellar surface patterns. Static water contact angle measurement revealed that surface hydrophilicity of these spin-coated thin films increases with increasing PEG block content.

Introduction

Amphiphilic block copolymers have attracted considerable attention in both fundamental and applied research for their unique chemical structure and physical properties. Driven by immiscibility of different blocks and packing restraint imposed by the connectivity of each block, amphiphilic block copolymers can form a variety of heterophasic morphologies in nanometer scales ranging from spheres to cylinders to lamellae.[1−3] Morphology and dimension could be tailored by manipulating the volume fraction of each block, copolymer molecular weight, monomer−monomer interaction and fabricating temperature. Taking advantage of their amphiphilic property, these nanostructures could find applications as a mask for nanolithography of inorganic materials and as a template for fabrication of nanoelectrode ensembles.[4−6] On the other hand, in selective solvent, amphiphilic block copolymers can self-assemble into micelles or vesicles with potential application for nanoreactors, drug delivery, and templates for synthesis of mesoporous materials and nanoparticles.[7−10]

Poly(ethylene glycol) (PEG), as a hydrophilic and biocompatible polyether, has been widely used in biomedical research and application due to its low toxicity and nonimmunogenicity as well as its ability to minimize protein adsorption to surfaces.[11] With biodegradability as a desirable feature, amphiphilic block copolymers consisting of biodegradable aliphatic polyester such as poly(L-lactide) (PLLA), polycaprolactone (PCL), and polyglycolide (PGA) as hydrophobic block and biocompatible PEG as hydrophilic block are particularly attractive for biological and pharmaceutical study.[12] Huh et al. have prepared PLLA-*alt*-PEG block copolymer through coupling reaction between dicarboxylated PLLA and PEG in the presence of dicyclohexyl carbodiimide and *N*-(dimethylamino)pyridine.[12a] They reported some unique properties of these copolymers, such as temperature-dependent swelling and optical transmittance, and improved mechanical properties. Reversible sol−gel transition exhibited by aqueous solutions of PEG-PLLA-PEG triblock copolymers has been studied by Kim et al., and thermosensitive biodegradable hydrogels consisting of these copolymers have further been developed.[12b] Biodegradable vesicles formed through spontaneous self-assembly of amphiphilic PCL-PEG diblock copolymer with potential application for sustained drug release have been reported by Ghoroghchian et al.[8a]

Different from the above synthetic aliphatic polyesters, optically active biodegradable poly[(*R*)-3-hydroxybutyrate] (PHB) is produced by many microorganisms as an intracellular carbon and energy storage material.[13] Due to its natural origin, PHB can be obtained in exceptionally pure form without retaining any catalyst; consisting entirely *R* units, natural PHB exhibits

* To whom correspondence should be addressed at the Division of Bioengineering, Faculty of Engineering, NUS. Phone: +65-6516-7273. Fax: +65-6872-3069. E-mail: bielj@nus.edu.sg.

† IMRE.

‡ Faculty of Science.

§ Faculty of Engineering.

10.1021/bm060675f CCC: $33.50
Published on Web 10/24/2006

relatively higher crystallinity and stronger hydrophobicity but lower glass transition temperature (T_g, ~5 °C) and lower in vivo degradation rate in comparison with synthetic aliphatic polyesters.[14] Generally, annealing at temperature higher than T_g is required for block copolymer to form equilibrium heterophasic morphology with reduced occurrence of unwanted grain boundaries and other defects.[15] This annealing could be avoided with PHB block copolymer with such lower T_g. Lower T_g is also preferred for drug delivery application, which is beneficial to the permeability of the incorporated drug; A lower in vivo degradation rate is required for biomedical or environmental applications where higher stability is desired. Therefore, biodegradable and biocompatible PHB has attracted much attention lately with its potential environmental, pharmaceutical, and biomedical applications.[16] It is expected that amphiphilic block copolymers consisting of PHB as hydrophobic block and PEG as hydrophilic block will have novel properties.

Recently, we reported the synthesis and characterization of PEG-PHB-PEG triblock copolymers, and their self-aggregation behavior in aqueous solution was also studied by using dynamic and static light scattering.[17] Our results indicate that micelles formed from PEG-PHB-PEG triblock copolymer through self-assembly process in water are quite stable and temperature-insensitive. This behavior is quite different from that of micelles prepared from synthetic aliphatic polyester/PEG block copolymers which are temperature-sensitive and thermally induced gelation is always observed.[12b] Poly(PHB/PEG urethanes) with improved mechanical properties and hydrophilicity in comparison with natural PHB have also been reported.[18] Herein, we report the synthesis and characterization of biodegradable amphiphilic PHB-*alt*-PEG block copolymers with well-defined alternating structure prepared from PHB-diol and PEG-diacid through coupling reaction. Their chemical structure and molecular characteristics have been studied by gel permeation chromatography (GPC), ^{1}H nuclear magnetic resonance (NMR), and Fourier transform infrared (FTIR); phase separated structures of these copolymers were investigated by differential scanning calorimetry (DSC), X-ray diffraction (XRD), and FTIR. While the surface morphology of thin films of diblock or triblock copolymers with high molecular weight has been studied extensively,[4−6] study on alternating block copolymers has received relatively less attention, especially on block copolymer containing biodegradable polyester blocks. Thus, the surface morphology of spin-coated PHB-*alt*-PEG block copolymer thin films on freshly cleaved mica were visualized by atomic force microscopy (AFM).

Experimental Section

Materials. Natural source poly[(*R*)-3-hydroxybutyrate] (PHB) was purchased from Aldrich and purified by dissolving in chloroform followed by filtration and subsequent precipitation in hexane. The M_n and M_w of purified PHB are 8.7×10^4 and 2.3×10^5, respectively. Poly(ethylene glycols) (PEGs) with M_n of ca. 2000 and 3400 were purchased from Aldrich and purified by dissolving in methylene chloride followed by precipitation in diethyl ether and further dried under high vacuum at 35 °C for 48 h before use. Their M_n and M_w were found to be 1960 and 2060, 3250 and 3380, respectively. Poly(ethylene glycol) bis(carboxymethyl) ether with M_n of ca. 600 was obtained from Aldrich and used without further purification. Bis(2-methoxyethyl) ether (diglyme, 99%), ethylene glycol (99%), dibutyltin dilaurate (95%), 1,3-*N*,*N*′-dicyclohexylcarbodiimide (DCC, 99%), 4-(dimethylamino)pyridine (DMAP, 99%), succinic anhydride (97%), triethylamine (99%), methanol, diethyl ether, 1,4-dioxane, and methylene chloride were purchased from Aldrich. Diglyme was dried with molecular sieves, and methylene chloride was dried by distilling over CaH_2 prior to use.

Telechelic hydroxylated PHB (PHB-diol) prepolymers were prepared through transesterification between natural source PHB and ethylene glycol with dibutyltin dilaurate as catalyst in diglyme, and telechelic carboxylated poly(ethylene glycol) (PEG-diacid) prepolymers were prepared by reaction of PEG with succinic anhydride in the presence of DMAP and triethylamine in 1,4-dioxane, as reported previously.[17a,19]

Synthesis of PHB-*alt*-PEG Block Copolymers. PHB-*alt*-PEG block copolymers were synthesized from PHB-diol and PEG-diacid at equal molar amounts through reaction between the hydroxyl group from PHB-diol and the carboxylic acid group from PEG-diacid in the presence of DMAP and DCC in dried methylene chloride. Typically, in a 250 mL Schlenk flask fitted with magnetic stirrer and decanter, 232 mg (0.103 mmol) of PEG-diacid with M_n of 2250, 282 mg (0.103 mmol) of PHB-diol with M_n of 2740, and 6.6 mg (0.054 mmol) of DMAP were loaded and dried under high vacuum at 40 °C overnight. Then, 30 mL of freshly dried methylene chloride was added to the flask to dissolve the above mixture followed by distilling off 20 mL of methylene chloride, which was repeated three times. Thus, any trace water in the system was removed through azeotropic distillation with 5 mL of methylene chloride left in the flask. At room temperature, 0.35 mL (1 M, 0.35 mmol) of DCC dissolved in methylene chloride was syringed in. After stirring under dry nitrogen for 2 days at room temperature, the reaction was stopped by adding 20 mL of methylene chloride. Precipitated dicyclohexylurea was filtered off, and the transparent filtrate was then precipitated in diethyl ether. Precipitate was collected through filtration followed by drying in high vacuum. The complete coupling reaction is indicated by observation of a unimodal peak with no low molecular weight fraction in the GPC curve of the dried product. The desired block copolymers were further purified two times by precipitating in a diethyl ether and methanol mixture (95/5, v/v). Yield: 0.31 g (58.7%). GPC (THF): $M_n = 11\,600$, $M_w/M_n = 1.59$. ^{1}H NMR (400 MHz, $CDCl_3$): δ 1.27 (d, -OCH(CH_3)-CH_2CO_2-), 2.41−2.60 (m, -OCH(CH_3)CH_2CO_2-), 2.66 (s, -$COCH_2CH_2CO$-), 3.64 (s, -OCH_2CH_2O- of PEG block), 4.24 (m, -OCH_2CH_2OCO-), 4.29 (s, -$COOCH_2CH_2OCO$-), 5.25 (m, -OCH(CH_3)CH_2CO_2-).

Molecular Characterization. GPC analysis was carried out with a Shimadzu SCL-10A and LC-8A system equipped with two Phenogel 5μ 50 and 1000 Å columns (size: 300 × 4.6 mm) in series and a Shimadzu RID-10A refractive index detector. Tetrahydrofuran (THF) was used as eluate at a flow rate of 0.30 mL/min at 40 °C. Monodispersed poly(ethylene glycol) standards were used to obtain a calibration curve.

The ^{1}H NMR spectra were recorded on a Bruker AV-400 NMR spectrometer at 400 MHz at room temperature. The ^{1}H NMR measurements were carried out with an acquisition time of 3.2 s, a pulse repetition time of 2.0 s, a 30° pulse width, 5208 Hz spectral width, and 32K data points. The chemical shift was referred to the solvent peaks (δ = 7.3 ppm for $CHCl_3$).

FTIR spectra of the polymer films cast on a KBr pellet were recorded on a Bio-Rad 165 FT-IR spectrophotometer; 64 scans were signal-averaged with a resolution of 2 cm^{-1} at room temperature.

DSC measurements were performed using a TA Instruments 2920 differential scanning calorimeter equipped with an autocool accessory and calibrated using indium. The following protocol

Scheme 1. Synthesis of PEG-diacids, PHB-diols, and PHB-*alt*-PEG Block Copolymers

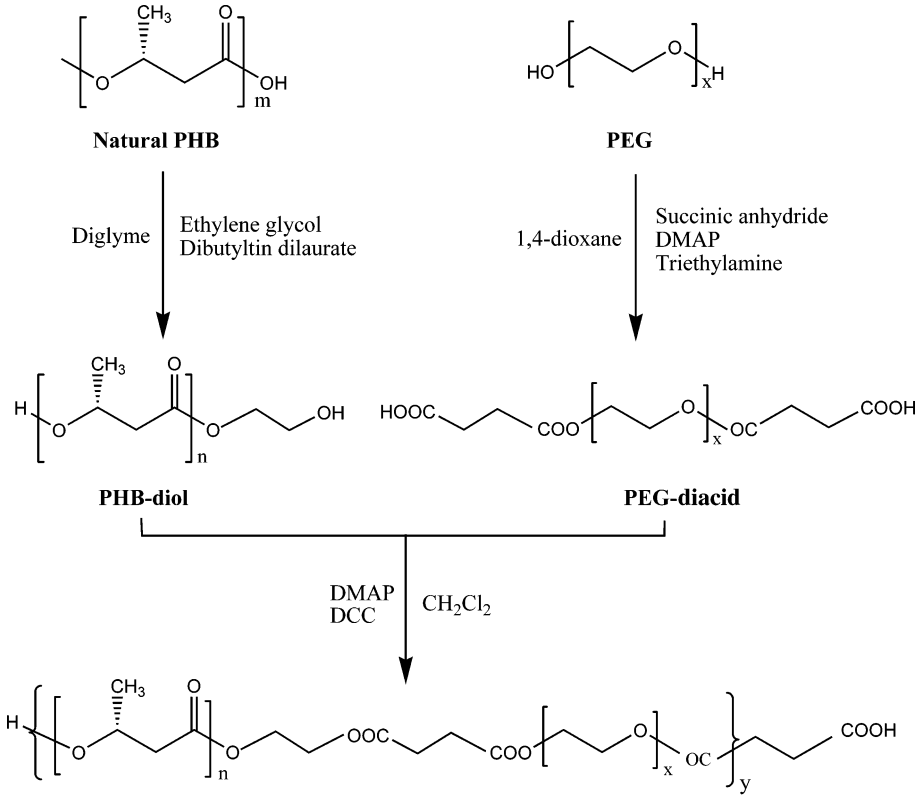

was used for each sample: heating from room temperature to 170 °C at 20 °C min^{-1}, holding at 170 °C for 2 min, cooling from 170 to −30 °C at 5 °C min^{-1}, and finally reheating from −30 to 170 °C at 5 °C min^{-1}. Data were collected during the second heating run. Peak maxima were taken as transition temperatures.

Wide-angle XRD measurements were carried out by using a Bruker GADDS diffractometer with an area detector operating under Cu Kα (1.5418 Å) radiation (40 kV, 40 mA) at room temperature. Film samples were mounted on a sample holder with double-sided adhesive tape.

Atomic Force Microscopy. Thin films of PHB-*alt*-PEG block copolymer were prepared by spin-coating their 1,2-dichloroethane solutions (2 mg/mL) onto freshly cleaved mica at a spinning speed of 1000 rpm and then dried overnight at room temperature. Residual solvent was completely removed by vacuum-drying for over 24 h at room temperature. Film thicknesses were determined by purposely applying a scratch to the polymer film and subsequent scanning by using Tencor P-10 Surface Profiler at 20 μm/s. The averaged film thickness was found to be 12 nm with all prepared films. The surface morphologies of these thin films were imaged by AFM (Nanoscope IIIa, Digital Instruments, USA) under ambient condition using tapping mode. Height and phase images were recorded simultaneously at a scan rate of 1.5 Hz. The AFM tips (PPP−NCH, Nanoscience Instruments, Inc., USA) used had a typical tip radius of 7 nm or less, and the cantilevers had a resonance frequency of 204−497 kHz. The height and width of the observed lamellar structures were measured from height images, and eighteen measurements were averaged with each sample.

Static Water Contact Angle Measurement. PHB-*alt*-PEG block copolymer thin films coated on freshly peeled mica were prepared according to the same way as that described above. Then, their static water contact angles were measured by the sessile method at 25 °C in an air atmosphere using a NRL-100-00-(230) contact angle goniometer (Ramè-Hart Inc., NJ). The telescope with magnification power of 23× was equipped with a protractor of 1° graduation. For each contact angle reported, at least five readings from different parts of the film surface were averaged. Each angle reported was reliable to 2°.

Results and Discussion

Synthesis and Molecular Characterization of PHB-*alt*-PEG Block Copolymers. PHB-*alt*-PEG block copolymers were synthesized according to the procedures presented in Scheme 1. First, telechelic hydroxylated PHB with M_n of 1740 or 2740 as determined by GPC was converted from high-molecular-weight natural source PHB through transesterification reaction with ethylene glycol in the presence of dibutyltin dilaurate in diglyme. At the same time, telechelic carboxylated poly(ethylene glycol) with M_n of 2250 or 3500 was prepared by reaction of PEG with succinic anhydride in the presence of DMAP and triethylamine in 1,4-dioxane. Then a coupling reaction between the hydroxyl group from PHB-diol and the carboxylic acid group from PEG-diacid in the presence of DMAP and DCC in dried methylene chloride leads to the formation of PHB-*alt*-PEG block copolymers. The molar ratio between PHB-diol and PEG-diacid was fixed at 1:1 to ensure as high a molecular weight of PHB-*alt*-PEG block copolymer as possible. Due to its moisture-sensitive nature, any trace water in the system was removed through azeotropic distillation, and the reaction was carried out under a nitrogen atmosphere. Finally, the desired PHB-*alt*-PEG block copolymers were purified from the reaction mixture by repeated precipitation in a diethyl ether and methanol mixture (95/5, v/v). A series of PHB-*alt*-PEG block copolymers with various PHB and PEG block lengths were synthesized, and the

Table 1. Molecular Characteristics of PHB-*alt*-PEG Block Copolymers

PHB-*alt*-PEG copolymers[a]	M_n[b] ($\times 10^3$)	M_w[b] ($\times 10^3$)	M_w/M_n[b]	PHB content (wt %) NMR[c]	PHB content (wt %) TGA[d]	yield (%)
HE(1740-600)	12.0	22.8	1.90	76.8	76.0	81.1
HE(1740-2250)	16.9	27.3	1.61	49.3	51.9	62.5
HE(1740-3500)	18.9	31.2	1.65	35.6	37.0	79.0
HE(2740-600)	7.8	10.9	1.39	84.6	83.8	80.9
HE(2740-2250)	11.6	18.5	1.59	62.5	63.1	58.7
HE(2740-3500)	11.6	15.8	1.36	43.7	46.1	65.0

[a] PHB-*alt*-PEG block copolymers are denoted as HE, and the numbers in parentheses show the indicative molecular weight of the respective precursor in grams per mole. [b] Determined by GPC. [c] Calculated from ^{1}H NMR results. [d] Calculated from TGA results.

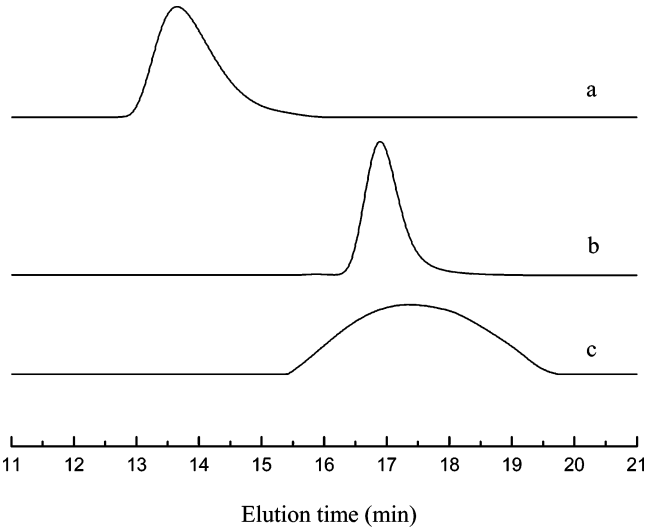

Figure 1. GPC curves of HE(1740-2250) block copolymer (a) and its precursors PEG-diacid ($M_n = 2250$) (b) and PHB-diol ($M_n = 1740$) (c).

obtained block copolymers are denoted as HE with the numbers in brackets showing the indicative molecular weight of respective precursor in grams per mole. The yield of such block copolymers changes from 60 to 80%, as shown in Table 1. The relatively low yield is due to removal of PHB-*alt*-PEG block copolymer with shorter PHB block during purification.

GPC analysis was carried out to determine the molecular weights and molecular weight distributions of PHB-*alt*-PEG block copolymers, and the results are listed in Table 1. The typical GPC traces for one purified PHB-*alt*-PEG block copolymer and its corresponding precursors are shown in Figure 1. Compared to those of corresponding precursors, a unimodal peak at relatively shorter elution time is observed in the GPC trace of purified PHB-*alt*-PEG block copolymer with nonoverlapping nature with those of corresponding precursors. This indicates that no precursor remains in purified block copolymer. The relatively narrower molecular weight distribution of PHB-*alt*-PEG block copolymers compared to their PHB-diol precursor is mostly likely due to removal of block copolymer with shorter PHB block during purification, as discussed above.

The chemical structure of PHB-*alt*-PEG block copolymers was verified by ^{1}H NMR spectroscopy, in which all proton signals belonging to both PHB and PEG blocks are confirmed. Figure 2 shows the ^{1}H NMR spectrum of HE(1740-2250) in $CDCl_3$ as a typical example. As shown in the spectrum of HE(1740-2250), the signals attributed to PHB block are observed at $\delta = 1.27$ (d, -OCH(CH_3)CH_2CO_2-), 2.41−2.60 (m, -OCH(CH_3)CH_2CO_2-), and 5.25 ppm (m, -OC*H*(CH_3)-CH_2CO_2-), and the signals to PEG block are observed at $\delta = 3.64$ ppm (s, -OCH_2CH_2O-). The signals at $\delta = 2.66$, 4.24, and 4.29 ppm are attributed to the linking group of COCH_2CH_2-CO, OCH_2CH_2OCO-, and COOCH_2CH_2OCO between PEG block and PHB block, respectively. The compositions of PHB-*alt*-PEG block copolymers could be calculated by comparing the integration value of resonances at $\delta = 5.25$ ppm assigned to methine in repeating units of PHB block and that at $\delta = 3.64$ ppm assigned to methylene in repeating units of PEG block, which are listed in Table 1. As shown in Table 1, the composition values determined by ^{1}H NMR are in good agreement with those calculated from two-step thermal degradation of block copolymers during thermogravimetric analysis (TGA). Figure S1 (Supporting Information) shows a typical TGA curve of PHB-*alt*-PEG block copolymer together with its corresponding precursors. The apparent improvement on thermal stability of PHB block and PEG block in PHB-*alt*-PEG block copolymer in comparison with their corresponding precursors as indicated by the increase of initial decomposition temperature observed in TGA is believed to be due to the reduction of the hydroxyl group and the carboxylic acid group upon coupling reaction.

Figure 3 shows the FTIR spectrum of HE(1740-2250) together with its corresponding precursors as a typical example. As shown in Figure 3b, the characteristic C−O−C stretching vibration of the repeated -OCH_2CH_2- units in PEG-diacid is observed at 1102 cm^{-1}, and the bands at 963 and 843 cm^{-1} are characteristic of the crystalline phase of PEG-diacid.[20] An intensive carbonyl stretching band at 1723 cm^{-1} characterizes the FTIR spectrum of pure PHB-diol as shown in Figure 3c.[17a] The observation of all characteristic absorptions for both PEG-diacid and PHB-diol in the spectrum of PHB-*alt*-PEG block copolymer, as shown in Figure 3a, verifies the formation of PHB-*alt*-PEG block copolymer. The decreased intensity of bands at 963 and 843 cm^{-1} in the spectrum of HE(1740-2250) in comparison with those in the spectrum of pure PEG-diacid is due to the lower crystallinity of PEG block in HE(1740-2250). Figure 4 shows the expansion of carbonyl stretching region of FTIR spectra for PHB-diol ($M_n = 1740$) and HE(1740-2250). The carbonyl stretching band characterizing PHB-diol can be resolved into an intensive band at 1723 cm^{-1} and a weak shoulder at 1736 cm^{-1}, corresponding to the carbonyl stretching band of crystalline PHB and amorphous PHB, respectively.[21] While the intensity of the band at 1723 cm^{-1} decreases, the intensity of the shoulder at 1736 cm^{-1} increases in the spectrum of HE(1740-2250) compared to that of pure PHB-diol, indicating the decrease of the crystallinity of the PHB block in PHB-*alt*-PEG block copolymers. The lower crystallinity of both PEG block and PHB block in PHB-*alt*-PEG block copolymer is believed due to the mutual interference from each other on their crystallization, which is also observed in DSC and XRD studies in the following sections.

PHB, as a natural biodegradable biopolyester produced by microorganisms, can undergo hydrolytic degradation and has shown good tissue biocompatibility.[14b] A copolymer of PHB with PEG shall be biodegradable because of the biodegradability of the PHB segments. For example, we recently synthesized poly(PHB/PEG urethanes) where the PHB and PEG blocks are linked with urethane linkage.[18a] The studies of hydrolytic degradation of the poly(PHB/PEG urethanes) under physiological conditions showed that the copolymers are biodegradable, undergoing random chain scission of the PHB blocks, and the degradation rate varies with the PHB/PEG ratio.[18b] The PHB-*alt*-PEG block copolymers synthesized in this work are expected

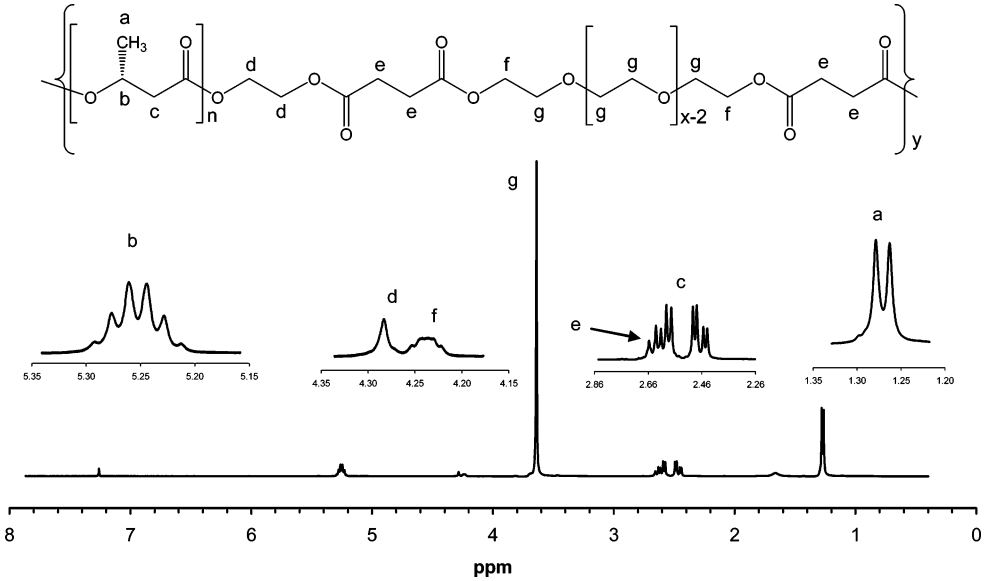

Figure 2. 400 MHz ^{1}H NMR spectrum of HE(1740-2250) block copolymer in $CDCl_3$.

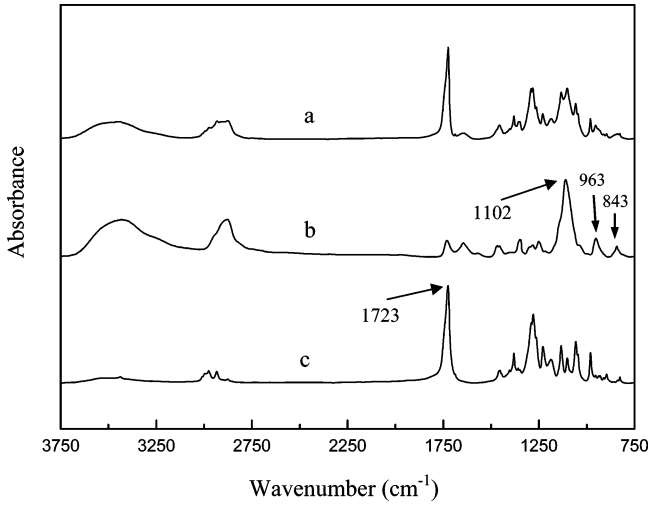

Figure 3. FTIR spectra of HE(1740-2250) block copolymer (a) and its precursors PEG-diacid (M_n = 2250) (b) and PHB-diol (M_n = 1740) (c).

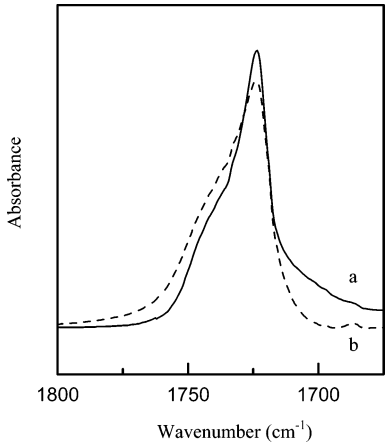

Figure 4. Expansions of the FTIR spectra of PHB-diol (M_n = 1740) (a) and HE(1740-2250) block copolymer (b).

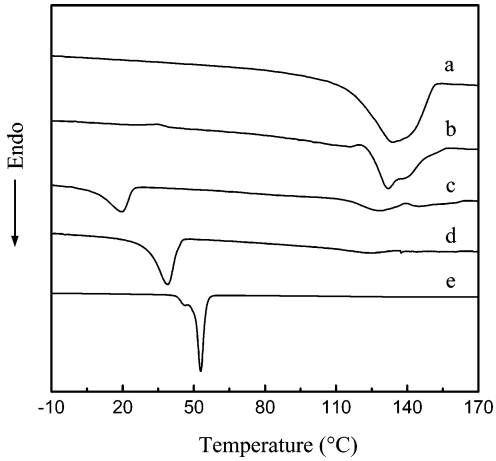

Figure 5. DSC curves of PHB-diol (M_n = 1740) (a), HE(1740-600) (b), HE(1740-2250) (c), HE(1740-3500) (d), and PEG-diacid (M_n = 3500) (e) in the second heating-up run.

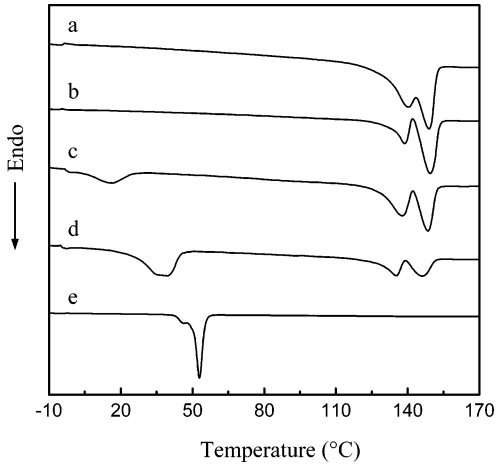

Figure 6. DSC curves of PHB-diol (M_n = 2740) (a), HE(2740-600) (b), HE(2740-2250) (c), HE(2740-3500) (d), and PEG-diacid (M_n = 3500) (e) in the second heating-up run.

to be biodegradable in a similar way (detailed studies are underway).

Crystallization Behaviors. Crystallization behavior of PHB block and PEG block in PHB-*alt*-PEG block copolymers has been investigated by using DSC. Figures 5 and 6 show the DSC heating curves of PHB-*alt*-PEG block copolymers synthesized in this study and their precursors after cooling at 5 °C min^{-1} from 170 °C, and the numerical values corresponding to thermal

Table 2. Melting Transition Temperatures, Corresponding Enthalpies, and Crystallinity for PHB-*alt*-PEG Block Copolymers

PHB-*alt*-PEG copolymers[a]	T_m[b] (°C)		ΔH_m[c] (J/g)		X_c[d] (%)	
	PEG	PHB	PEG	PHB	PEG	PHB
PHB-diol (M_n 1740)		135.0		96.6		65.9
PHB-diol (M_n 2740)		150.0		96.0		65.5
PEG-diacid (M_n 2250)	44.8		127.5		62.2	
PEG-diacid (M_n 3500)	52.9		143.4		69.9	
HE(1740-600)		131.9		68.0		46.4
HE(1740-2250)	19.9	128.9	46.6	50.4	22.7	34.4
HE(1740-3500)	41.3	117.6	76.1	27.4	37.1	18.7
HE(2740-600)		149.3		75.1		51.2
HE(2740-2250)	15.7	148.5	28.4	68.2	13.9	46.5
EH(2740-3500)	40.1	146.0	76.0	63.4	37.1	43.2

[a] PHB-*alt*-PEG block copolymers are denoted as HE, and the numbers in parentheses show the indicative molecular weight of the respective precursor in grams per mole. [b] Melting point determined in DSC second heating-up run. For PHB block having multipeak due to melting−recrystallization, the T_m value for the second peak is given. [c] Enthalpy change during melting transition determined in DSC second heating-up run. $\Delta H_m = \Delta H_i/W_i$, where ΔH_i is the area of the endothermic peak for PEG or PHB block read from DSC curves and W_i is the weight fraction of the corresponding block. [d] Crystallinity calculated from melting enthalpies. Reference values of 205.0 and 146.6 J/g for completely crystallized PEG and PHB were used, respectively.[17a]

transition and crystallinity of each block are listed in Table 2. Both PEG and PHB are crystalline polymers.[13,20] While PEG-diacid exhibits a sharp and strong melting peak centered at 45 or 53 °C determined by its molecular weight (Figures 5e and 6e), a broad melting peak centered at 135 or 150 °C is observed for PHB-diol with M_n of 1740 or 2740, respectively (Figures 5a and 6a). The structured melting behavior corresponding to the PHB crystalline phase observed for PHB-diol with M_n of 2740 and its block copolymers is probably due to successive melting and recrystallization of regions with imperfect crystallinity. For PHB-*alt*-PEG block copolymers, except HE(1740-600) and HE(2740-600), both the PHB melting transition and the PEG melting transition are observed, as shown in Figures 5c,d and 6c,d, indicating formation of a separated PHB crystalline phase and PEG crystalline phase in PHB-*alt*-PEG block copolymers. However, in comparison with those of PHB or PEG precursors, the melting transition of PHB block or PEG block shifted to lower temperature with lower crystallinity calculated from the melting endothermal enthalpy and weight fraction of the corresponding block, and the difference was found to be dependent on the molecular weight of PHB block or PEG block. As an example, the melting transition temperature (T_m) of the PHB crystalline phase decreases from 135 °C with a crystallinity (X_c) of 65.9% for PHB-diol (M_n = 1740) to 131.9 °C with X_c of 46.4% for HE(1740-600) and further to 117.6 °C with X_c of 18.7% for HE(1740-3500) with increasing M_n of the PEG block. The lowered X_c and T_m of PHB blocks or PEG blocks compared to those of their corresponding precursors are believed to be due to the mutual interference from each other. It has been demonstrated before that PHB and PEG are miscible in the melting phase.[22] Then, when PHB-*alt*-PEG block copolymer is cooled from its molten state, the crystallization of PHB blocks is restricted because of the interference coming from existing PEG blocks. On the other hand, after PHB blocks solidify and crystallize first at higher temperature, PEG blocks are excluded and confined between PHB lamellae. Thus, the mobility of PEG segments is hindered, and its crystallization is restricted. The absence of PEG melting transition for HE(1740-600) and HE(2740-600) is because that PEG block with such small molecular weight is unable to crystallize within the measurement temperature range.

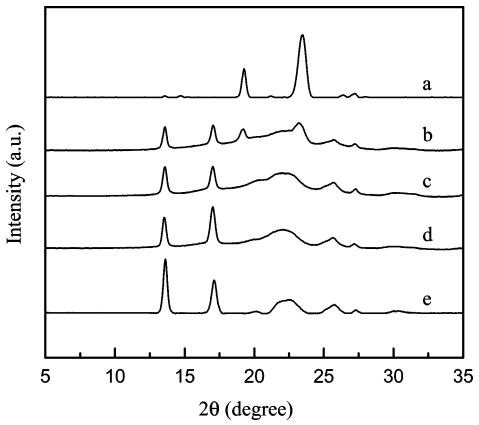

Figure 7. XRD patterns of PEG-diacid (M_n = 3500) (a), HE(1740-3500) (b), HE(1740-2250) (c), HE(1740-600) (d), and) PHB-diol (M_n = 1740) (e).

The crystallization behavior of PHB block and PEG block was also studied by using XRD measurement. The XRD patterns of PHB-diol (M_n, 1740), PEG-diacid (M_n, 3500), and PHB-*alt*-PEG block copolymers with identical PHB-diol (M_n = 1740) but different PEG-diacid (M_n increased from 600 to 3500) are shown in Figure 7 as typical examples. The observation of characteristic reflection peaks of crystalline PHB at $2\theta = 13.6$ and 17.0° in XRD patterns of PHB-*alt*-PEG block copolymers (Figure 7b−d) indicates the formation of PHB crystalline phase as in pure PHB-diol (Figure 7e). The decrease in relative intensity of these two peaks with increasing M_n of PEG block in PHB-*alt*-PEG block copolymers is due to the interference from PEG block as discussed above. The characteristic reflection peaks of crystalline PEG are observed at $2\theta = 19.3$ and 23.5°, as shown in Figure 7a. These two characteristic reflection peaks appear in the XRD pattern for HE(1740-3500), indicating that the separated PEG crystalline phase is formed coexisting with the PHB crystalline phase. No obvious observation of characteristic reflection peaks for crystalline PEG in the XRD patterns for other PHB-*alt*-PEG block copolymers indicates that PEG block is unable to crystallize at the measurement temperature of 25 °C when M_n of PEG block is 2250 or below under the interference from PHB block. The XRD results are in good agreement with those obtained in DSC studies.

Morphology Studies. The surface morphology of PHB-*alt*-PEG block copolymer thin films spin-coated on freshly cleaved mica substrate was investigated by AFM using the tapping mode. Figure 8 shows the height and phase images of the HE-(1740-3500) block copolymer film surface as a typical example. As shown in Figure 8a, an array of laterally regular lamellar structure perpendicular to the substrate plane is seen at the surface of the block copolymer film. Similar features in the height image and its phase image (Figure 8b) indicate the observed topography is due to phase separation. The thickness of the film measured by using the Tencor P-10 Surface Profiler is ~12 nm. Usually, with ultrathin film coated on a substrate from block copolymer as in the present study, the surface morphology of the film is often determined by the surface wetting property of the substrate surface.[23] It is well-known the mica surface is preferentially wetted by hydrophilic PEG rather than by hydrophobic PHB. Therefore, we hypothesize that the preferential wetting of the mica surface by PEG block from alternating PHB-*alt*-PEG block copolymer leads to the formation of lamellar structure with both PHB block and PEG block exposed to air/polymer interface generating spatially periodic domains with different chemical constituents of block copolymer in the direction parallel to the substrate plane. The

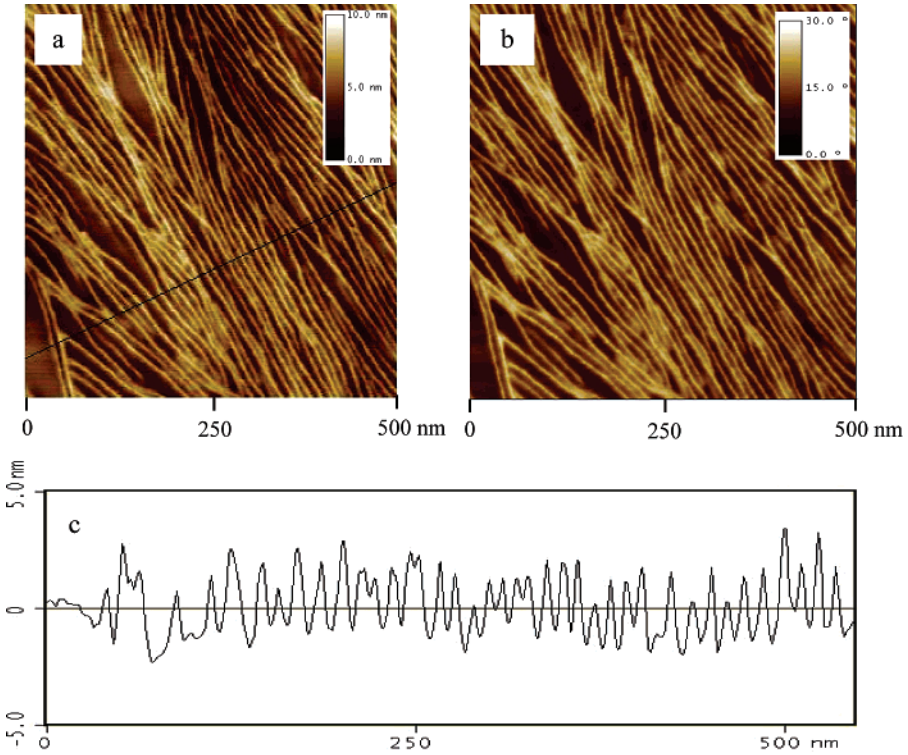

Figure 8. AFM height image (a), phase image (b), and height profile measured along the black line marked in the height image (c) of HE(1740-3500) block copolymer thin film. The height and phase scales are shown in the inset. Image sizes are 500 nm × 500 nm.

low T_g (~5 °C) of PHB facilitates achievement of the laterally regular morphology, avoiding thermal annealing at higher temperature as required by other block copolymers.[15] We have studied the surface morphology of PEG-PHB-PEG triblock copolymer thin films spin-coated on mica prepared according to the same method, and only island-holes (Figure S2 of the Supporting Information) was visualized instead of regular lamellar structure due to edge dislocation of the triblock copolymer thin film as reported previously.[24] In contrast, such edge dislocation is assumed to be retarded by confinement from the alternatively connected blocks. Thus, the well-defined alternating structure of PHB-*alt*-PEG block copolymer is essential for the formation of lamellar structure. Comparison between the height image and its phase image obtained simultaneously indicates the lighter phase corresponds to hard PHB domains and the darker phase corresponds to soft PEG domains. The averaged width of PHB domains measured from height image analysis by cross-sectional method as shown in Figure 8c is ~9.7 nm, which is comparable to the theoretical PHB block length of ~6.9 nm calculated by assuming a helical structure of PHB block with M_n of 1740.[25] This indicates the PHB block adopts a stretched structure in block copolymer thin films. The height difference between PHB domains and its neighboring PEG domains is ~2.9 nm, as measured in Figure 8c. Similar surface morphology has been observed with other PHB-*alt*-PEG block copolymer thin films, and the width of PHB domains is determined by PHB block length. For example, as calculated PHB block length increases from ~6.9 nm with HE(1740-3500) to ~9.5 nm with HE(2740-3500) by assuming a helical structure of PHB block, the width of PHB domains increases from ~9.7 nm with HE(1740-3500) to ~11.8 nm with HE(2740-3500), which further confirms the stretched helical structure of PHB block in such block copolymer ultrathin film.

The static water contact angle of the spin-coated thin films has been measured to determine their surface hydrophilicity. As typical examples, Figure 9 shows the static water contact angles of PHB-diol (M_n = 1740 or 2740) and some PHB-*alt*-PEG block copolymers with varied weight fraction of PEG block. As shown in Figure 9, while the contact angle of PHB-diol is ~60° independent of its molecular weight in the present study, the static water contact angle of PHB-*alt*-PEG block copolymers decreases to lower value with increasing weight fraction of PEG block, indicating more PEG block has migrated to the thin film surface in the presence of water due to its water soluble property. This property is essential when these block copolymers are employed as surface modifier to retard unwanted attachment of protein or cells or as a template to prepare inorganic patterned materials. Utilizing the intrinsic selectivity of PEG blocks toward various metal ions, PHB-*alt*-PEG block copolymer thin films can therefore be used to direct chemical reagents to an interface mirroring the pattern of the polymer template.

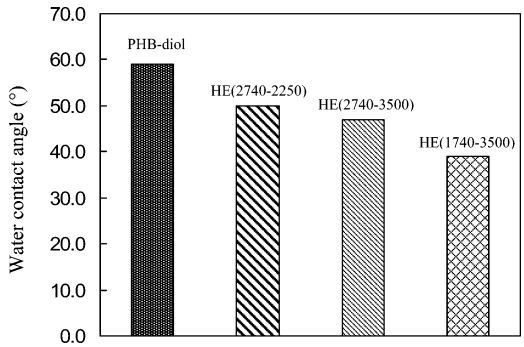

Figure 9. Static water contact angles of PHB-diol (M_n = 1740 or 2740) and PHB-*alt*-PEG block copolymers with varied weight fraction of PEG block.

Conclusions

A series of novel biodegradable amphiphilic alternating block copolymer PHB-*alt*-PEG have been successfully synthesized

through coupling reaction between hydroxyl group from PHB-diol and the carboxyl acid group from PEG-diacid in the presence of DCC and DMAP in dried methylene chloride. Their chemical structures have been verified by GPC, ^{1}H NMR, and FTIR studies. GPC analysis suggested a complete reaction took place leading to formation of PHB-*alt*-PEG block copolymer with relatively narrow molecular weight distributions. ^{1}H NMR results showed the PHB block content in PHB-*alt*-PEG block copolymer ranged from 35 to 85% in weight, which is in good agreement with those calculated from the two-step thermal decomposition procedure in TGA analysis.

Microphase-separated structures of PHB-*alt*-PEG block copolymer were studied by DSC, XRD, and FTIR. DSC results indicated that both PHB block and PEG block in PHB-*alt*-PEG block copolymer can aggregate together to form separate crystalline phases, except HE(1740-600) and HE(2740-600) with too short PEG block (M_n 600) in which only the PHB crystalline phase is formed. However, the melting transitions of both PHB and PEG crystalline phases shift to lower temperature with lower crystallinity which is due to the effect of mutual interference from each other on their crystallization. The decrease in melting point or crystallinity is determined by the molecular weights of PHB block and PEG block. Such restricted crystallization of both PHB block and PEG block was also observed in XRD studies and FTIR analysis.

The surface morphology of PHB-*alt*-PEG block copolymer thin films has been visualized by AFM using the tapping mode. Due to the preferential wetting of mica by PEG block and low T_g of PHB block, the laterally regular lamellar structure of PHB-*alt*-PEG block copolymer thin films perpendicular to the mica surface is formed without application of any externally applied guiding fields. Detailed studies on the surface morphology influenced by crystalline phases of both blocks, the surface property of the underlying substrate, and film thickness are underway. Static water contact angle measurement indicated the PEG block preferentially migrates to the thin film surface, which is essential for subsequent selective chemical reaction on the nanometer scale as a template for preparation of inorganic patterned materials.

Acknowledgment. The authors acknowledge financial support from the Agency for Science, Technology and Research (A*STAR) and the National University of Singapore (NUS). The authors greatly thank Prof. Kam W. Leong of the Department of Biomedical Engineering, Duke University, for his valuable suggestions and helpful discussions.

Supporting Information Available. Experimental details and supplementary figures. This material is available free of charge via the Internet at http://pubs.acs.org.

References and Notes

(1) Hamley, I. W. *The physics of block copolymers*; Oxford University Press: Oxford, U.K., 1998.
(2) (a) Xu, C.; Fu, X. F.; Fryd, M.; Xu, S.; Wayland, B. B.; Winey, K. I.; Composto, R. J. *Nano Lett.* **2006**, *6*, 282−287. (b) Kim, S. H.; Misner, M. J.; Xu, T.; Kimura, M.; Russell, T. P. *Adv. Mater.* **2004**, *16*, 226−231. (c) Fustin, C. A.; Lohmeijer, G. G.; Duwez, A. S.; Jonas, A. M.; Schubert, U. S.; Gohy, J. F. *Adv. Mater.* **2005**, *17*, 1162−1165.
(3) (a) Ishizone, T.; Han, S.; Hagiwara, M.; Yokoyama, H. *Macromolecules* **2006**, *39*, 962−970. (b) Senshu, K.; Kobayashi, M.; Ikawa, N.; Yamashita, S.; Hirao, A.; Nakahama, S. *Langmuir* **1999**, *15*, 1763−1769.
(4) (a) Fasolka, M. J.; Mayes, A. M. *Annu. Rev. Mater. Res.* **2001**, *31*, 323−355. (b) Pai, R. A.; Humayun, R.; Schulberg, M. T.; Sengupta, A.; Sun, J. N.; Watkins, J. J. *Science* **2004**, *203*, 507−510.
(5) (a) Cheyne, R. B.; Moffitt, M. G. *Langmuir* **2005**, *21*, 10297−10300. (b) Jain, A.; Hall, L. M.; Garcia, C. B. W.; Gruner, S. M.; Wiesner, U. *Macromolecules* **2005**, *38*, 10095−10100. (c) Kim, D. H.; Kim, S. H.; Lavery, K.; Russell, T. P. *Nano Lett.* **2004**, *4*, 1841−1844.
(6) Hirota, K.; Tajima, K.; Hashimoto, K. *Langmuir* **2005**, *21*, 11592−11595.
(7) (a) Li, Y. B.; Deng, Y. H.; Tong, X. L.; Wang, X. G. *Macromolecules* **2006**, *39*, 1108−1115. (b) He, Y. Y.; Li, Z. B.; Simone, P.; Lodge, T. P. *J. Am. Chem. Soc.* **2006**, *128*, 2745−2750.
(8) (a) Ghoroghchian, P. P.; Li, G. Z.; Levine, D. H.; Davis, K. P.; Bates, F. S.; Hammer, D. A.; Therien, M. J. *Macromolecules* **2006**, *39*, 1673−1675. (b) Saviæ, R.; Luo, L. B.; Eisenberg, A.; Maysinger, D. *Science* **2003**, *300*, 615−618. (c) Battaglia, G.; Ryan, A. J. *J. Am. Chem. Soc.* **2005**, *127*, 8757−8764.
(9) (a) Duxin, N.; Liu, F. T.; Vali, H.; Eisenberg, A. *J. Am. Chem. Soc.* **2005**, *127*, 10063−10069. (b) Sakai, T.; Alexandridis, P. *J. Phys. Chem. B* **2005**, *109*, 7766−7777.
(10) (a) Kataoka, K.; Harada, A.; Nagasaki, Y. *Adv. Drug Delivery Rev.* **2001**, *47*, 113−131. (b) Riess, G. *Prog. Polym. Sci.* **2003**, *28*, 1107−1170. (c) Bao, X. Y.; Zhao, X. S.; Li, X.; Chia, P. A.; Li, J. *J. Phys. Chem. B* **2004**, *108*, 4684−4689. (d) Bao, X. Y.; Zhao, X. S.; Li, X.; Li, J. *Appl. Surf. Sci.* **2004**, *237*, 380−386.
(11) Herold, D. A.; Keil, K.; Bruns, D. E. *Biochem. Pharmacol.* **1989**, *38*, 73−76.
(12) (a) Huh, K. M.; Bae, Y. H. *Polymer* **1999**, *40*, 6147−6155. (b) Kim, S. W.; Leong, B.; Bae, Y. H.; Lee, D. S. *Nature (London)* **1997**, *388*, 860−862. (c) Guan, J. J.; Sacks, M. S.; Beckman, E. J.; Wagner, W. R. *Biomaterials* **2004**, *25*, 85−96. (d) Wan, Y. Q.; Chen, W. N.; Yang, J.; Bei, J. Z.; Wang, S. G. *Biomaterials* **2003**, *24*, 2195−2203.
(13) Doi, Y. *Microbial polyester*; VCH: New York, 1990.
(14) (a) Abe, H.; Doi, Y. *Biomacromolecules* **2002**, *3*, 133−138. (b) Gogolewski, S.; Jovanovic, M.; Perren, S. M.; Dillon, J. G.; Hughes, M. K. *J. Biomed. Mater. Res.* **1993**, *27*, 1135−1148.
(15) (a) Sivaniah, E.; Hayashi, Y.; Matsubara, S.; Kiyono, S.; Hashimoto, T.; Fukunaga, K.; Kramer, E. J.; Mates, T. *Macromolecules* **2005**, *38*, 1837−1849. (b) Albrecht, T. T.; Schotter, J.; Kästle, G. A.; Emley, N.; Shibauchi, T.; Elbaum, L. K.; Guarini, K.; Black, C. T.; Tuominen, M. T.; Russell, T. P. *Science* **2000**, *290*, 2126−2129.
(16) (a) Anderson, A. J.; Dawes, E. A. *Microbiol. Rev.* **1990**, *54*, 450−472. (b) Müller, H. M.; Seebach, D. *Angew. Chem., Int. Ed. Engl.* **1993**, *32*, 477−502. (c) Lenz, R. W.; Marchessault, R. H. *Biomacromolecules* **2005**, *6*, 1−8.
(17) (a) Li, J.; Li, X.; Ni, X. P.; Leong, K. W. *Macromolecules* **2003**, *36*, 2661−2667. (b) Li, X.; Mya, K. Y.; Ni, X. P.; He, C. B.; Leong, K. W.; Li, J. *J. Phys. Chem. B* **2006**, *110*, 5920−5926. (c) Li, J.; Ni, X. P.; Li, X.; Tan, N. K.; Lim, C. T.; Ramakrishna, S.; Leong, K. W. *Langmuir* **2005**, *21*, 8681−8685. (d) Li, J.; Li X.; Ni, X.; Wang, X.; Li, H.; Leong, K. W. *Biomaterials* **2006**, *27*, 4132−4140.
(18) (a) Li, X.; Loh, X. J.; Wang, K.; He, C. B.; Li, J. *Biomacromolecules* **2005**, *6*, 2740−2747. (b) Loh, X. J.; Tan, K. K.; Li, X.; Li, J. *Biomaterials* **2006**, *27*, 1841−1850.
(19) Hirt, T. D.; Neuenschwander, P.; Suter, U. W. *Macromol. Chem. Phys.* **1996**, *197*, 1609−1614.
(20) Bailey, J. L.; Koleske, J. V. *Poly(ethylene oxide)*; Academic Press: New York, 1976.
(21) Li, X.; Li, J.; Leong, K. W. *Macromolecules* **2003**, *36*, 1209−1214.
(22) You, J. W.; Chiu, H. J.; Don, T. M. *Polymer* **2003**, *44*, 4355−4362.
(23) (a) Cheng, K. W.; Chan, W. K. *Langmuir* **2005**, *21*, 5247−5250. (b) Morkvad, T. L.; Lopes, W. A.; Hahm, J.; Sibener, S. J.; Jaeger, H. M. *Polymer* **1998**, *39*, 3871−3875. (c) Xuan, Y.; Peng, J.; Cui, L.; Wang, H. F.; Li, B. Y.; Han, Y. C. *Macromolecules* **2004**, *37*, 7301−7307.
(24) (a) Mansky, P.; Tsui, O. K. C.; Russell, T. P.; Gallot, Y. *Macromolecules* **1999**, *32*, 4832−4837. (b) Liu, Y.; Rafailovich, M. H.; Sokolov, J.; Schwarz, S. A.; Bahal, S. *Macromolecules* **1996**, *29*, 899−906. (c) Coulon, G.; Ausserre, D.; Russell, T. P. *J. Phys. (Paris)* **1990**, *51*, 777−786.
(25) Pazur, R. J.; Hocking, P. J.; Raymond, S.; Marchessault, R. H. *Macromolecules* **1998**, *31*, 6585−6592.

BM060675F